


ORIGINAL RESEARCH ARTICLE

SNX9 determines the surface levels of integrin $\beta 1$ in vascular endothelial cells: Implication in poor prognosis of human colorectal cancers overexpressing SNX9

Kazufumi Tanigawa^{1,2*} | Masashi Maekawa^{2,3*}  | Takeshi Kiyoi⁴ | Jun Nakayama⁵ | Riko Kitazawa^{6,7} | Sohei Kitazawa⁶ | Kentaro Semba⁵ | Tomohiko Taguchi⁸ | Satoshi Akita¹ | Motohira Yoshida¹ | Kei Ishimaru¹ | Yuji Watanabe¹ | Shigeki Higashiyama^{2,3}

¹Department of Gastrointestinal Surgery and Surgical Oncology, Ehime University Graduate School of Medicine, Ehime, Japan

²Department of Biochemistry and Molecular Genetics, Ehime University Graduate School of Medicine, Ehime, Japan

³Division of Cell Growth and Tumor Regulation, Proteo-Science Center, Ehime University, Ehime, Japan

⁴Division of Analytical Bio-medicine, Advanced Research Support Center, Ehime University, Ehime, Japan

⁵Department of Life Science and Medical Bioscience, School of Advanced Science and Engineering, Waseda University, Tokyo, Japan

⁶Department of Molecular Pathology, Ehime University Graduate School of Medicine, Ehime, Japan

⁷Division of Diagnostic Pathology, Ehime University Hospital, Ehime, Japan

⁸Department of Integrative Life Sciences, Graduate School of Life Sciences, Tohoku University, Sendai, Japan

Correspondence

Masashi Maekawa and Shigeki Higashiyama, Division of Cell Growth and Tumor Regulation, Proteo-Science Center, Ehime University Shitsukawa, Toon, 791-0295 Ehime, Japan. Email: masashim@m.ehime-u.ac.jp (M.M.); shigeki@m.ehime-u.ac.jp (S.H.)

Funding information

YOKOYAMA Foundation for Clinical Pharmacology, Grant/Award Number: Research Grant 2017 (YRY-1703) to MM; JSPS, Grant/Award Numbers: KAKENHI/JP18K16317 to KT, KAKENHI/JP16H046980 to SH, KAKENHI/JP18K15244 to MM

Abstract

Angiogenesis, the formation of new blood vessels, is involved in a variety of diseases including the tumor growth. In response to various angiogenic stimulations, a number of proteins on the surface of vascular endothelial cells are activated to coordinate cell proliferation, migration, and spreading processes to form new blood vessels. Plasma membrane localization of these angiogenic proteins, which include vascular endothelial growth factor receptors and integrins, are warranted by intracellular membrane trafficking. Here, by using a siRNA library, we screened for the sorting nexin family that regulates intracellular trafficking and identified sorting nexin 9 (SNX9) as a novel angiogenic factor in human umbilical vein endothelial cells (HUVECs). SNX9 was essential for cell spreading on the Matrigel, and tube formation that mimics in vivo angiogenesis in HUVECs. SNX9 depletion significantly delayed the recycling of integrin $\beta 1$, an essential adhesion molecule for angiogenesis, and reduced the surface levels of integrin $\beta 1$ in HUVECs. Clinically, we showed that SNX9 protein was highly expressed in tumor endothelial cells of human colorectal cancer tissues. High-level expression of SNX9

Abbreviations: BM, basement membrane; CUL3, cullin-3; EGFR, epidermal growth factor receptor; GEO, Gene Expression Omnibus; HUVEC, human umbilical vein endothelial cell; PM, plasma membrane; SNX, sorting nexin; VE-cadherin, vascular endothelial-cadherin; VEGF, vascular endothelial growth factor; VEGFR, vascular endothelial growth factor receptor.

*Tanigawa and Maekawa have equally contributed to this work.

This is an open access article under the terms of the Creative Commons Attribution-NonCommercial License, which permits use, distribution and reproduction in any medium, provided the original work is properly cited and is not used for commercial purposes.

© 2019 The Authors. *Journal of Cellular Physiology* Published by Wiley Periodicals, Inc.

messenger RNA significantly correlated with poor prognosis of the patients with colorectal cancer. These results suggest that SNX9 is an angiogenic factor and provide a novel target for the development of new antiangiogenic drugs.

KEYWORDS

angiogenesis, colorectal cancer, endothelial cells, integrin β 1, sorting nexin 9

1 | INTRODUCTION

One of the hallmarks in the development of solid tumors is tumor angiogenesis, the process of new blood vessel growth in tumor tissues from the pre-existing vasculatures (Folkman, 1971; Hida, Maishi, Annan, & Hida, 2018). The angiogenic activity of endothelial cells arises in response to various growth factors such as vascular endothelial growth factor (VEGF) and hepatocyte growth factor released from the neighboring tumor cells (Carmeliet & Jain, 2011). By receiving a variety of stimuli including VEGF, the endothelial cells lining the inner layer of blood vessels drastically change their characteristics (e.g., growth, motility, adhesion, cell–cell contact), leading to angiogenesis (Potente, Gerhardt, & Carmeliet, 2011). Tumor angiogenesis is critical for not only the tumor growth beyond a few millimeters in size by the supply of nutrients and oxygen but also the tumor metastasis by providing the passage to other tissues (Maishi & Hida, 2017). Thus, the inhibition of angiogenesis can suppress tumor growth and metastasis (Folkman, 1971). Among the complicated molecular mechanisms of angiogenesis, VEGF-dependent proliferative signals through the vascular endothelial growth factor receptors (VEGFRs) have been attractive targets for developing the anticancer drugs (Ferrara & Adami, 2016). To date, antiangiogenic drugs such as bevacizumab (humanized monoclonal antibody for VEGF-A) and sunitinib (tyrosine kinase inhibitor of VEGFRs) have been successfully developed and used to cure cancers (e.g., colorectal cancer, lung cancer, and renal cell carcinoma; Clarke & Hurwitz, 2013).

Among a variety of solid tumors, colorectal cancers exhibit high tumor angiogenic activities (Mathonnet et al., 2014). In fact, bevacizumab is administrated as first or second line treatment of colorectal cancer, which is highly effective (De Falco, 2014). In the randomized phase III study of the metastatic colorectal cancer therapy combination with oxaliplatin, the progression-free survival and overall survival were 9.4 months and 21.3 months in the bevacizumab-treated group, and 8.0 months and 19.9 months in the placebo group (Saltz et al., 2008). Despite the good efficacy of bevacizumab in treating colorectal cancer, the development of drug resistance after long-term administration often poses a major challenge (Bergers & Hanahan, 2008; Lupo et al., 2016). In addition, the anti-VEGF antibodies and VEGFR inhibitors occasionally cause hypertension and gastrointestinal perforation as side effects (de Jesus-Gonzalez, Robinson, Moslehi, & Humphreys, 2012; Sliesoraitis & Tawfik, 2011). To overcome these issues, the development of novel antiangiogenic drugs targeting molecular machinery instead of the VEGF/VEGFR axis is required.

During the complicated multistep angiogenesis, endothelial cells receive stimulations through transmembrane proteins (e.g., VEGFRs, Notch ligands, Notch receptors, vascular endothelial-cadherin, integrins) on their cell surface, leading to proper angiogenic responses (Horowitz & Seerapu, 2012; Kandachar & Roegiers, 2012). The localization of these membrane proteins in the plasma membrane (PM) is balanced by the rate of their endocytosis from the PM to the endosomes and their recycling from the endosomes to the PM (Mellman & Yarden, 2013). The manipulation of membrane trafficking of these angiogenic cargos in endothelial cells could inhibit angiogenesis (Maes, Olmeda, Soengas, & Agostinis, 2016). Thus, we aimed to identify novel angiogenic molecules involved in the intracellular membrane trafficking, which could be targeted for the development of new antiangiogenic drugs.

In this study, by utilizing the siRNA library for the sorting nexin (SNX) family, which regulates a variety of intracellular membrane trafficking processes, we found that sorting nexin 9 (SNX9) was essential for the tube formation that mimics *in vivo* angiogenesis of human umbilical vein endothelial cells (HUVECs). SNX9 was essential for determining the surface levels of integrin β 1 as well, suggesting a possible molecular mechanism by which SNX9 regulates tube formation. In patients with human colorectal cancer, SNX9 was highly expressed in the tumor endothelial cells. Our results suggest that SNX9 is a novel angiogenic factor that regulates the recycling of integrin β 1.

2 | MATERIALS AND METHODS

2.1 | Antibodies

The following antibodies were purchased from the manufacturers as indicated: rabbit anti-SNX9 antibody (HPA031410; dilution 1:1000 for western blot analysis; dilution 1:750 for immunohistochemistry; Sigma, Tokyo, Japan), rabbit anti-SNX5 antibody (ab180520; dilution 1:1000; Abcam, Tokyo, Japan), rabbit anti-CD31 antibody (ab28364; dilution 1:100 for immunohistochemistry; Abcam), goat anti-integrin β 1 antibody (N-20, dilution 1:1000 for western blot analysis; Santa Cruz, Dallas, TX), mouse anti-integrin β 1 antibody (P5D2, dilution 1:1000; R&D systems, Minneapolis, MN), mouse anti-integrin β 1 antibody (TS2/16, dilution 1:500 for western blot analysis and immunofluorescence; Biolegend, San Diego, CA), Alexa488-conjugated mouse anti-integrin β 1 antibody (TS2/16, dilution 1:200; BioLegend), mouse anti-GAPDH antibody (5A12, dilution 1:6000; Wako, Tokyo, Japan), mouse anti-Myc antibody (9E10; dilution 1:1000; Santa Cruz), HRP-conjugated anti-mouse-IgG antibody (W4021; dilution 1:2000; Promega, Tokyo, Japan), horse radish peroxidase (HRP)-conjugated anti-rabbit-IgG

antibody (W4011; dilution 1:2000; Promega, Tokyo, Japan), HRP-conjugated anti-goat-IgG antibody (V805A; dilution 1:2000; Promega), goat Alexa488-conjugated anti-mouse-IgG antibody (A11001; dilution 1:2000; Molecular Probes, Eugene, OR), and goat Alexa568-conjugated anti-mouse-IgG antibody (A11004; dilution 1:2000; Molecular Probes).

2.2 | Plasmids

Myc-SNX9 was amplified from a vector containing the human SNX9 complementary DNA (cDNA; a kind gift from Ms. Yuki Tanaka, Ehime University) using the following pairs of primers: 5'-ATGGAACAAAAAC TCATCTCAGAAGAGGATCTGATGGCCACCAAGGCTCGGGT-3' (Myc-SNX9 sense primer) and 5'-CTACATCACTGGAAAGCGGC-3' (SNX9 antisense primer). The PCR product was introduced into the blunt end of the CSII-CMV-MCS-IRES2-Bsd vector. GFP-Rab5, GFP-Rab7, GFP-Rab11, or LAMP1-GFP in the CSII-CMV-MCS-IRES2-Bsd vector (Maekawa et al., 2017) were used for the co-localization experiments. Full length and the LC-PX domain of SNX9 were amplified from the vector containing the human SNX9 cDNA using the following pairs of primers: 5'-ATGGCCACCAAGGCTCGGGT-3' (SNX9 sense primer), 5'-CTACATCACTGGAAAGCGGC-3' (SNX9 antisense primer), 5'-GAC TACGTTGAAATTTTACC-3' (LC-PX sense primer), and 5'-CTATCG GAAATTTAGGAACT-3' (LC-PX antisense primer). The PCR products were introduced into the blunt end of the pEU-N-bls vector. Bls-SNX9 (Δ LC) was generated with the following pairs of primers: 5'-ACTTTTG ACTGTGTGGTAGCAGATC-3' (sense primer) and 5'-TGTGGGAACCAG CCCTCGTTCTCTCT-3' (antisense primer).

2.3 | Cell culture

HUVECs were purchased from Cell Systems (Kirkland, WA) and Lonza (Tokyo, Japan). HUVECs were maintained at 37°C with 5% CO₂ in EBM-2 (Lonza) according to the manufacturer's instructions. HUVECs at passage 2–4 were used for experiments. HEK293T cells were maintained at 37°C with 5% CO₂ in Dulbecco's modified Eagle's medium (Wako) supplemented with 10% fetal bovine serum (FBS), 20 units/ml penicillin, and 100 µg/ml streptomycin.

2.4 | Transfection

Transfections of siRNAs (25 nM) into HUVECs were performed using RNAimax (Invitrogen, Tokyo, Japan) according to the manufacturer's instructions. Subsequent experiments were performed at 72 hr posttransfection. Transfection of plasmids into HEK293T cells was performed using GeneJuice (Millipore, Burlington, MA) according to the manufacturer's instructions.

2.5 | Small interfering RNAs

The following validated siRNA duplex oligomers were purchased and used for the knockdown experiments: GUUGCAAGCUGAGAUGAAU (siSNX9 #1; Sigma), CAUCGAAUAUCAGCUAACA (siSNX9 #2; Sigma), GAAUGUAAUCACGAGUAUA (siSNX9 #3; Sigma), GGGACUUUGUA

TABLE 1 List of human SNX genes and siRNA duplex oligomers used for siRNA screening

SNX gene	Sequence of siRNA duplex targeting the SNX genes
SNX1	GACAUUGAGUGGUGCUGGU
SNX2	GGAAGAUGCUCAAAUUACU
SNX3	GACUUAUUAUGAUUGAUAA
SNX4	CUCACUAUGGCGGCGAUU
SNX5	CAGUAAAGAUCCGCAACUUU
SNX6	CUGCUAAGGAUCUCCUGUA
SNX7	GAAAGAAUUGGCCCAAUU
SNX8	GGAUGUGCAGAAACAAGUUA
SNX9	GUUGCAAGCUGAGAUGAAU
SNX10	CAAUUCACAAGUUUGCCUU
SNX11	CUGAGUUUCUGCAGGUCAU
SNX12	GACAAACCUACCUAUCUUC
SNX13	GAGUUUCGGCUCAACUUGA
SNX14	CACAAUUUCUUGAUAAAGAU
SNX15	CCCAGAGGAUGUCAAGAG
SNX16	GUGAACAGAUCCUAAAGGU
SNX17	GCUUUUAGCUCAGACGGUA
SNX18	GACUUCUUCUUAAGCGCA
SNX19	CUCAUAACCUGUUGAGUA
SNX20	CUGAGGAGAUGAUCUGUGA
SNX21	CAGAUUGCCAGCCAGCCCA
SNX22	CUGAUCAGUCCAGAGGCCU
SNX23	GGCUUAAUACCUCGGAUCU
SNX24	GUGAUAGUACAUUCUGAAA
SNX25	GCAACUAAGGUUAUCAAUUU
SNX26	CACAUUCAGCUCCUGCUGU
SNX27	CUCUACAUUCAGAAUUUAU
SNX28	GCGCGUGUUGGAAACGUCA
SNX29	GAGAGAACGAGGUGUCUAA
SNX30	GACUAGAGAUCUCUUCGUU
SNX31	GUAAGCUAGCUGCUGAGA
SNX32	CAGACAUGCUGAGGUACUA
SNX33	CAUCAGAGCUGGUGCGUAA

Note. siRNA: small interfering RNA; SNX: sorting nexin.

GAGAAUUU (siSNX9 #4 targeting the 3'-UTR of the human SNX9 messenger RNA (mRNA); Sigma; Bendris, Williams, et al., 2016). The list of SNX genes and siRNA duplex oligomers (Sigma) used for the siRNA screening are shown in Table 1. Control siRNA was purchased from Sigma (SIC-001).

2.6 | Lentiviral expression

Lentiviruses carrying Myc-SNX9, GFP-Rab5, GFP-Rab7, GFP-Rab11, or LAMP1-GFP were produced by the transfection of those cDNA cloned in the CSII-CMV-MCS-IRES2-Bsd vector with two packaging vectors (the

pCAG-HIVgp vector and pCMV-VSVG-RSV-Rev vector) into HEK293T cells. At 48 hr posttransfection, the lentiviruses in the medium were collected. At 24 hr posttransfection of siRNA into HUVECs, the collected lentiviruses were added into the medium of the HUVECs. The expression of Myc-SNX9 and GFP-tagged organelle markers in HUVECs was detected at 48 hr post-lentiviral infection. The CSII-CMV-MCS-IRES2-Bsd, pCAG-HIVgp, and pCMV-VSVG-RSV-Rev vectors were kind gifts from Dr. Hiroyuki Miyoshi (RIKEN, Tokyo, Japan).

2.7 | Western blot analysis

Proteins were subjected to sodium dodecyl sulfate (SDS) polyacrylamide gel electrophoresis and transferred to polyvinylidene difluoride membranes (BioRad, Hercules, CA). After blocking of these membranes in 5% skim milk in 0.05%-Tween-20/TBS buffer, the membranes were incubated with the primary antibodies, followed by the secondary antibodies conjugated to peroxidase in 5% skim milk in 0.05%-Tween-20/TBS buffer. The proteins were visualized by enhanced chemiluminescence using a LAS-4000 (GE Healthcare, Tokyo, Japan). To detect integrin $\beta 1$ using TS2/16, the cell lysates were collected under nonreducing conditions. Except for the experiments using TS2/16, all the cell lysates were collected under reducing conditions.

2.8 | Immunofluorescence staining

Cells were fixed with 4% paraformaldehyde (PFA) in PBS for 30 min at room temperature and permeabilized with 0.1% Triton X-100 in PBS for 15 min at room temperature. After blocking with 3% bovine serum albumin (BSA) in PBS for 1 hr at room temperature, the cells were incubated with primary antibodies at 4°C overnight and then with secondary antibodies conjugated to fluorophores at room temperature for 1 hr. To stain the nuclei, the fixed cells were treated with Hoechst33342 (dilution 1:2000; Molecular Probes) at room temperature for 1 hr.

2.9 | Phalloidin staining

Cells were fixed with 4% PFA in PBS for 30 min at room temperature and permeabilized with 0.1% Triton X-100 in PBS for 15 min at room temperature. After blocking with 3% BSA in PBS for 30 min at room temperature, the cells were incubated with rhodamine-conjugated phalloidin (dilution 1:1000; Molecular Probes) for 1 hr at room temperature.

2.10 | Biotinylation assay

The biotinylation assays were performed as described previously (Maekawa et al., 2017). Briefly, the HUVECs were washed with ice-cold PBS two times followed by incubation with biotin solution (0.1 mg/ml; sulfo-NHS-biotin; Thermo Fisher Scientific; Tokyo, Japan) in 0.1 M Hepes; 0.15 M NaCl; pH 8.0) for 15 min at 4°C. After quenching with ice-cold serum-containing EBM-2 medium, the cells were subjected to immunoprecipitation. The cells were lysed in 0.5 ml of IP buffer (25 mM Tris-HCl; pH 7.4; 150 mM NaCl; 1%

NP-40; 1 mM EDTA; 5% glycerol) containing the complete protease inhibitors (Roche). After incubation of the cell lysates on ice for 10 min, the cell lysates were centrifuged at 10,000g for 10 min at 4°C. The resultant supernatants were incubated with streptavidin magnetic beads (Dynabeads M-280; Invitrogen) for 1 hr at 4°C. The beads were washed with IP buffer three times followed by the collection of proteins with SDS buffer without 2-mercaptoethanol. The total and biotinylated integrin $\beta 1$ were detected by western blot analysis using the TS2/16 antibody.

2.11 | Integrin $\beta 1$ uptake and recycling assays

The internalization and recycling assays of integrin $\beta 1$ were performed as described previously (Arjonen, Alanko, Veltel, & Ivaska, 2012). Briefly, integrin $\beta 1$ on the cell surface of HUVECs was labeled with Alexa488-conjugated TS2/16 antibody in the growth-EBM-2 medium containing 30 mM Hepes (pH 7.6) on ice for 1 hr. Cells were then washed with ice-cold PBS and the medium was replaced with fresh growth medium containing 30 mM Hepes (pH 7.6). For the internalization assay, the cells were incubated at 37°C with 5% CO₂ for the indicated time-point. After the internalization, the cells were put on the ice and the fluorescence on the cell surface was quenched by adding anti-Alexa488 antibody and incubating on ice for 1 hr. To monitor the recycling of integrin $\beta 1$, labeled integrin $\beta 1$ on the cell surface was allowed to internalize for 1 hr at 37°C with 5% CO₂ followed by quenching of the surface integrin $\beta 1$. Cells were incubated again at 37°C with 5% CO₂ for the indicated time-point. After incubation, the surface fluorescence signal of integrin $\beta 1$ was quenched again. For imaging, the cells were fixed with 4% PFA in PBS for 30 min at room temperature. The fluorescence intensity of Alexa488 excluding the background fluorescence intensity was quantified with ImageJ (NIH). The fluorescence intensities were normalized against the total surface staining (at 0 min before quenching, for the uptake assay) or total internalized staining (for the recycling assay).

2.12 | Transferrin uptake and recycling assays

The internalization and recycling assays of transferrin were performed as described previously (Lee et al., 2015). For the uptake assay, HUVECs were serum-starved in EBM-2 for 30 min at 37°C. The cells were then incubated with 50 μ g/ml of Alexa488-transferrin (Molecular Probes) in 0.15% serum-containing EBM-2 for 5 or 10 min at 37°C. The cells were then chilled on ice and incubated in acid-wash buffer (20 mM sodium-acetate buffer; 1 mM CaCl₂; 150 mM NaCl; pH 4.8) on ice for 5 min to remove Alexa488-transferrin in the PM. For the recycling assay, HUVECs were incubated in 0.15% serum-containing EBM-2 for 30 min at 37°C followed by incubation in 0.15% serum-containing EBM-2 containing 50 μ g/ml Alexa488-transferrin for 1 hr at 37°C. After washing with ice-cold PBS, the cells were incubated in the acid-wash buffer on ice for 5 min to remove the surface-bound Alexa488-transferrin. Cells were washed with ice-cold PBS and chased in growth-EBM-2 medium containing 400 μ g/ml unlabeled human holo-transferrin (Thermo Fisher Scientific) at 37°C with 5% CO₂. For imaging, the cells were fixed with 4% PFA in PBS at room temperature for 30 min. The fluorescence intensity

of Alexa488 excluding the background fluorescence intensity was quantified with ImageJ (NIH).

2.13 | Spreading and network formation on the Matrigel

HUVECs were collected by treatment with trypsin for 1 min followed by seeding on the Matrigel basement membrane (BD Matrigel™ Basement Membrane Matrix Growth Factor Reduced; BD Biosciences, Tokyo, Japan). The cells were then incubated in the growth-EBM-2 medium for 1 hr or 12 hr at 37°C with 5% CO₂. The cells were fixed and F-actin was stained with rhodamine-conjugated phalloidin. The cell size and network length were measured with ImageJ (NIH, Bethesda, MD).

2.14 | Tube formation assay

Collagen I gel was reconstituted by mixing Nitta gelatin Type I-A collagen gel (Nitta Gelatin; 180712), 10× 199 medium (Nitta Gelatin; 180517), reconstitution buffer (Nitta Gelatin; 181126, Osaka, Japan). HUVECs (0.5 × 10⁵ cells/well of 12 well plates) seeded on the reconstituted collagen I gel were subjected to siRNA transfection. At 6 hr post-siRNA transfection, the cells were packed with collagen I again, followed by the addition of 50 ng/mL VEGF-A (R&D Systems) in 0.15% serum and heparin-containing EBM-2 medium. Tube formation of HUVECs was observed at 66 hr after the addition of VEGF-A. The cells were fixed and F-actin was stained with rhodamine-conjugated phalloidin. The tube length was measured with ImageJ (NIH).

2.15 | Cell proliferation assay

The cell proliferation assay was performed as described previously (Murakami et al., 2019) with slight modifications. A total of 0.5 × 10⁵ HUVEC were seeded into a six-well plate in triplicate. Cells were treated with siRNA on the next day. After 48 hr, 0.5 × 10⁵ cells were replated into a 12-well plate in triplicate. On the next day, cells were then treated with the same siRNA again, and cultured in growth-EBM-2 medium with or without VEGF-A (50 ng/ml). The cells were counted at each time points after siRNA transfection.

2.16 | Cell migration assay

A total of 0.5 × 10⁵ HUVEC were seeded into collagen I-coated 35 mm dishes (IWAKI, Shizuoka, Japan). Cells were treated with siRNA on the next day. After 72 hr, the cell culture was scratched with a 1000 µl pipette tip, followed by incubation with growth-EBM-2 medium for 15 hr. Images were obtained using a microscope (Olympus, Tokyo, Japan), and analyzed with Fiji software (NIH).

2.17 | Confocal microscopy

Confocal microscopy was performed using the A1R laser confocal microscope (Nikon, Tokyo, Japan) with a 60× 1.27 Plan-Apochromat

water immersion lens or a 10× 0.45 Plan-Apochromat lens. Images were analyzed with ImageJ or Fiji software (NIH).

2.18 | Protein synthesis using wheat germ cell-free system

The transcription and translation for the production of biotinylated recombinant proteins were performed using WEPRO7240 Expression Kit (CellFree Science, Matsuyama, Japan), according to the manufacturer's instructions with slight modifications. The mRNA templates were generated by incubating for 6 hr at 37°C in a mixture containing 2 µl of 5× transcription buffer, 1 µl of 25 mM NTP mix, 0.1 µl of 80 U/µl RNase inhibitor, 0.1 µl of 80 U/µl SP6 RNA polymerase, 1 µg pEU vectors (Bls-SNX9, WT; Bls-SNX9, ΔLC; Bls-LC-PX) and RNase-free water (up to 10 µl). For cell-free translation of mRNA templates, the mixtures for lower and upper layer were prepared as follows: lower layer [6.25 µl of WEPRO7240, 0.25 µl of 20 µg/µl creatine kinase (Roche, Basel, Switzerland), 4.68 µl of 4× SUB-AMIX, 10 µl of mRNA templates, 1 µl of recombinant Bir-A (a kind gift from Dr. Hiroyuki Takeda, Ehime University), 1 µl of 12.5 µM D-biotin (Sigma), 1.82 µl of RNase-free water (total 25 µl)]; upper layer [31.25 µl of 4× SUB-AMIX, 5 µl of 12.5 µM D-biotin, 88.75 µl of RNase-free water (total 125 µl)]. The upper layer mixture was added to a well of 96-well flat bottom plate followed by the addition of the lower layer mixture into the bottom, carefully. The reaction mixtures were incubated for 24 hr at 16°C to produce recombinant proteins. The reaction mixtures (total 150 µl/well) were centrifuged at 10,000g for 10 min at 4°C. The resultant supernatants were subjected to western blot analysis to detect the production of recombinant proteins. The biotinylated proteins were detected using the VECTASTAIN ABC kit (Funakoshi, Tokyo, Japan).

2.19 | Immunohistochemistry and H&E staining

Immunohistochemical staining of colorectal cancer tissues was carried out as described previously (Kiyoi, 2018) with slight modifications. Briefly, the formaldehyde-fixed paraffin-embedded specimens were subjected to sectioning. Deparaffinized sections were incubated with 3% hydrogen peroxidase solution for 10 min at room temperature to block endogenous peroxidase activity followed by incubation with citrate buffer (pH 6.0) for 10 min at 120°C to retrieve the antigen. After blocking with 3% BSA in PBS for 30 min at room temperature, the sections were incubated with primary antibodies at 4°C overnight and then with the secondary antibody (Envision⁺; Dako, Tokyo, Japan) at room temperature for 45 min followed by the addition of DAB. The sections were also stained with hematoxylin for 1 min. For the validation of the anti-SNX9 antibody, 50 µl of crude biotinylated SNX9 recombinant proteins (WT, ΔLC, or LC-PX) and anti-SNX9 antibody (dilution 1:750) were pre-incubated in 200 µl of 3% BSA in PBS buffer at 4°C overnight. The mixture including the pre-absorbed antibody was used as the primary antibody for immunohistochemistry. Hematoxylin and eosin (H&E) staining of colorectal cancer tissues was carried out as described previously (Kiyoi, 2018). The stained specimens were observed using

the all-in-one fluorescence microscope BIOREVO BZ-9000 (KEYENCE, Tokyo, Japan). The images were analyzed with the BZ-II analyzer (KEYENCE) and Fiji (NIH). We defined epithelial and endothelial cells as SNX9-positive when the signals for the SNX9-DAB staining were positive above the threshold 90.

2.20 | Human colorectal cancer samples

All human colorectal cancer samples were collected from the archives of the Department of Molecular Pathology, Ehime University Graduate School of Medicine and Division of Diagnostic Pathology, Ehime University Hospital. Clinical and pathological information was obtained from the pathology records at Ehime University Hospital. This study was approved by the Institutional Review Board of Ehime University Hospital (approved IRB protocol number: 1611003). Informed consent was obtained from all subjects. All experiments were performed by following the approved study plan and relevant guidelines.

2.21 | Clinical database analysis

The survival analysis was performed by the Kaplan–Meier method on the patients with clinical colorectal cancer. We subjected Gene Expression Omnibus (GEO) datasets (accession number, GSE14333 and GSE17536) to survival analysis which was executed by the 'ggplot2', 'survminer,' and "survival" packages with R (ver. 3.4.1.). The GSE14333 (Jorissen et al., 2009) and GSE17536 (Smith et al., 2010) datasets contain the clinical status and expression data of SNX9 collected using the Affymetrix Human Genome U133 Plus 2.0 Array.

2.22 | Statistical analyses

Statistical analyses was carried out by the Student's two-tailed *t* test. The log-rank test in survival analysis was performed by the "survminer" package in R (ver. 3.4.1.).

3 | RESULTS

3.1 | A genetic screen to identify novel angiogenic factors using SNX siRNA library

We reasoned that the regulators of membrane trafficking are essential for angiogenesis. Sorting nexins (SNXs) are critical factors for a variety of intracellular membrane trafficking and the human genome possesses 33 SNX genes (Table 1; Cullen, 2008). To examine if SNXs regulate angiogenesis, we performed the siRNA screening against 33 SNX genes (Figure 1a,b). We found that SNX9 knockdown drastically inhibited the tube formations of HUVECs in an in vitro assay system that mimics in vivo angiogenesis (Arnaoutova & Kleinman, 2010; Figure 1a,b). The tube length of the SNX9-knockdown cells was reduced approximately 75% compared to that of the control cells (Figure 1b).

3.2 | SNX9 is required for tube formation of human umbilical vein endothelial cells

We next used multiple siRNA oligos to corroborate the involvement of SNX9 in tube formation in HUVECs. We transfected three different siRNA oligos targeting SNX9 and the knockdown efficiency was confirmed by western blot analysis (Figure 2a). The tube formation was significantly suppressed by SNX9 knockdown using the three different siRNA oligos (Figure 2b). The tube length of those SNX9-depleted cells was reduced approximately 75% compared to that of the control HUVECs (Figure 2b). Since we noticed that SNX9-knockdown HUVECs did not extend well on collagen I gels during the tube formation assay compared to the control cells (Figure 2b), we next examined the cell spreading activity on the Matrigel basement membrane (BM). One hour after seeding on the BD Matrigel™ BM, the control HUVEC spread and the size was approximately 1600 μm^2 (Figure 2c). In contrast, the cell shape of SNX9-knockdown HUVECs was still round and its cell size was approximately 400–800 μm^2 (Figure 2c). HUVECs form networks on the Matrigel upon long-time incubation, which also mimics in vivo angiogenesis (Ohnuki et al., 2012). As shown in Figure 2d, the control HUVECs formed networks upon incubation on the Matrigel for 12 hr. In contrast, by the knockdown of SNX9, the network formation by HUVECs on the Matrigel was drastically inhibited (Figure 2d). The network length was reduced approximately 80% by the depletion of SNX9 (Figure 2d). The expression of Myc-tagged siRNA-resistant SNX9 cDNA partially restored the inhibition of network formation in SNX9-knockdown HUVECs, excluding the off-target effect of siRNA (Figure 2e,f). Together, these data suggested that SNX9 is essential for angiogenesis in HUVECs.

3.3 | SNX9 regulates recycling of integrin $\beta 1$ from endosomes to the plasma membrane

We next sought to elucidate the mechanism by which SNX9 regulates tube formation in HUVECs. Integrin $\beta 1$, an adhesion molecule, is essential for angiogenesis and the reduction in the levels of integrin $\beta 1$ on the cell surface inhibits the cell spreading on the Matrigel (Hongu et al., 2015; Maekawa et al., 2017). Since we noticed that the cell spreading on the Matrigel in SNX9-knockdown HUVECs was drastically impaired (Figure 2c,d), we reasoned that the surface integrin $\beta 1$ would decrease by the depletion of SNX9. As expected, by staining HUVECs without membrane permeabilization, we found that the fluorescence intensity of integrin $\beta 1$ on cell surface was significantly decreased by the SNX9 knockdown (Figure 3a). The decrease in the surface levels of integrin $\beta 1$ by the SNX9 knockdown was also confirmed by biotinylation of the surface proteins (Figure 3b). Both experiments showed that the cell surface integrin $\beta 1$ levels were decreased to approximately 40–60% by the SNX9 knockdown. The population of surface integrin $\beta 1$ is controlled by endocytosis from the PM to endosomes and the recycling from endosomes to the PM (De Franceschi, Hamidi, Alanko, Sahgal, & Ivaska, 2015). Since total protein expression of integrin $\beta 1$ was not affected in the SNX9-knockdown

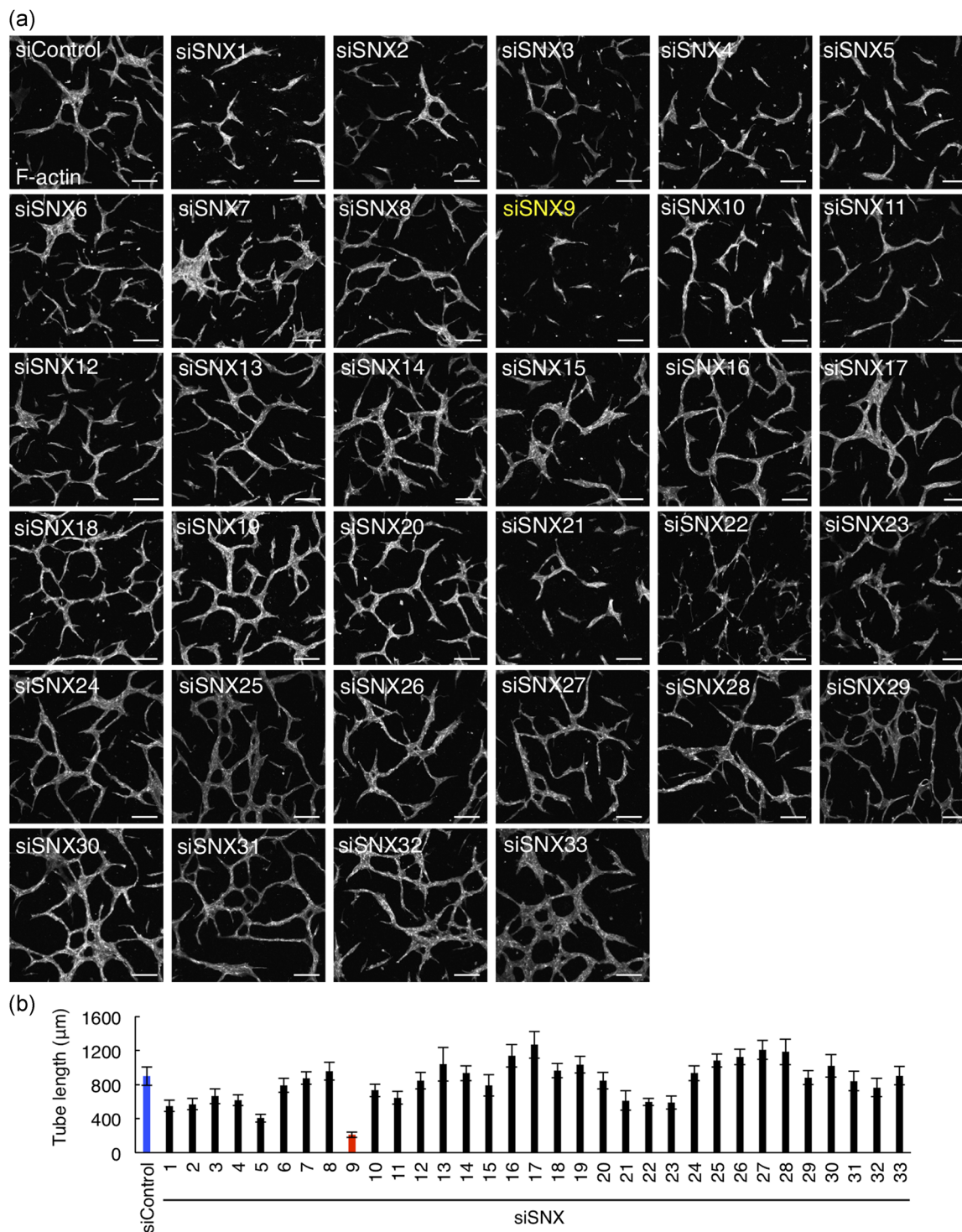


FIGURE 1 SNX siRNA screening to identify novel angiogenic factors in HUVECs. (a) Confocal images of tube formation. HUVECs seeded on collagen I gel were treated with the control or SNXs siRNA (SNX1-33) and packed on collagen I followed by VEGF stimulation for 66 hr. HUVECs were visualized by the staining of F-actin with rhodamine-labeled phalloidin. Bars, 200 μ m. (b) The quantitation of (a). A total of 10 tubes were analyzed. Data shows are the mean \pm SEM. The blue and red bars indicate the tube length of siControl- and siSNX9-treated HUVECs, respectively. HUVEC: human umbilical vein endothelial cells; SEM: standard error of mean; siRNA: small interfering RNA; SNX: sorting nexin; VEGF: vascular endothelial growth factor [Color figure can be viewed at wileyonlinelibrary.com]

HUVECs (Figure 3c), integrin β 1 would be relocalized from the PM to intracellular compartments by the SNX9 depletion. As expected, integrin β 1 was localized in intracellular punctate structures by the SNX9 knockdown, whereas, integrin β 1 localized in the PM in the

control HUVECs (Figure 3d). We then determined the integrin β 1-positive intracellular compartments in the cells depleted of SNX9. The co-localization analysis with several endocytic proteins (Rab5, early endosomes; Rab11, recycling endosomes; Rab7, late endosomes;

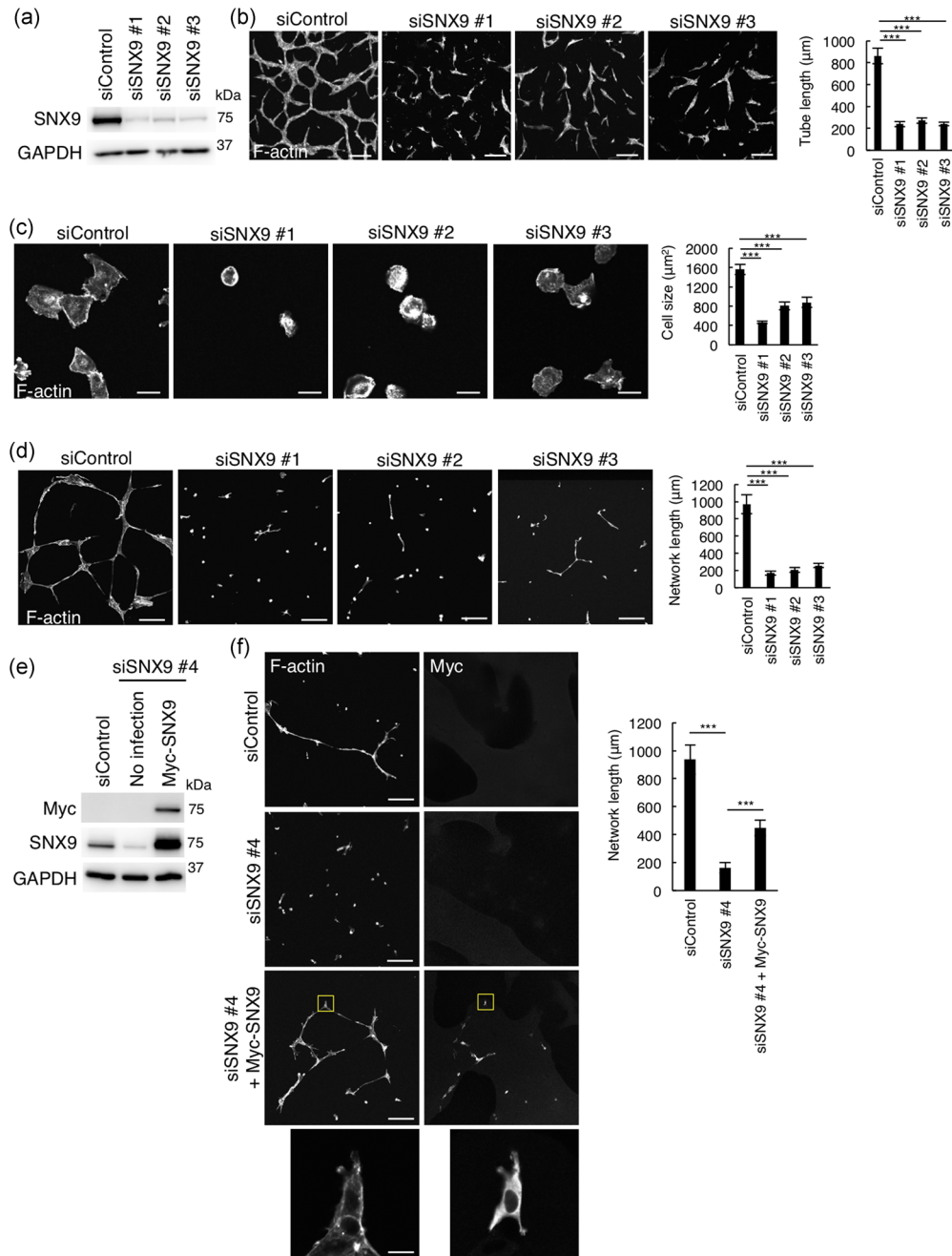


FIGURE 2 SNX9 is essential for tube formation in HUVECs. (a) Western blot analysis of HUVEC lysates 72 hr posttransfection of siRNAs. (b) Confocal images and quantitation of tube formation. HUVECs seeded on collagen I gel were treated with control, or SNX9 siRNAs (siSNX9 #1–#3) and packed on collagen I followed by VEGF stimulation for 66 hr. HUVECs were visualized by the staining for F-actin with rhodamine-labeled phalloidin. Bars, 200 μm . A total of 30 of the tubes from three independent experiments were analyzed. Data shows the mean \pm SEM. *** p < .001. (c) Confocal images and quantitation of cell spreading. HUVECs were seeded on the Matrigel followed by incubation for 1 hr. The cells were visualized by staining of F-actin with rhodamine-labeled phalloidin. Bars, 20 μm . The size of 50 cells from three independent experiments were analyzed. Data shown are the mean \pm SEM. *** p < .001. (d) Confocal images and quantitation of network formation. HUVECs were seeded on the Matrigel followed by incubation for 12 hr. The cells were visualized by staining for F-actin with rhodamine-labeled phalloidin. Bars, 200 μm . A total of 30 of networks from three independent experiments were analyzed. Data shown are the mean \pm SEM. *** p < .001. (e,f) Rescue experiments for SNX9 knockdown: (e) Western blot analysis of cell lysates of HUVECs infected with siRNA resistant-Myc-SNX9-carrying lentivirus. (f) Confocal images and quantitation of network formation of HUVECs infected with siRNA resistant-Myc-SNX9-carrying lentivirus (f). HUVECs were seeded on the Matrigel followed by incubation for 12 hr. Cells were visualized by the staining for F-actin with rhodamine-labeled phalloidin. The Myc-SNX9 was labeled with anti-Myc antibody. Bars, 200 μm . Magnifications of the squared areas are shown in the lower panels (bars, 20 μm). A total of 30 of the tubes from three independent experiments were analyzed. Data shown are the mean \pm SEM. *** p < .001. HUVEC: human umbilical vein endothelial cells; SEM: standard error of mean; siRNA: small interfering RNA; SNX9: sorting nexin 9; VEGF: vascular endothelial growth factor [Color figure can be viewed at wileyonlinelibrary.com]

LAMP1, lysosomes) indicated that integrin $\beta 1$ localized mostly to early endosomes/recycling endosomes in the SNX9-knockdown cells (Figure 3e). These data suggested that SNX9 functioned in not the degradation pathway but the recycling pathway of integrin $\beta 1$.

We then compared the trafficking of integrin $\beta 1$ in control and SNX9-depleted HUVECs. First, the internalization of integrin $\beta 1$ from the PM was measured. As shown in Figure 3f, the intensity of Alexa488-integrin $\beta 1$ after the 10-min chase was about 50% compared

to the fluorescence intensity on cell surface before chase in both the control and SNX9-knockdown cells. SNX9 knockdown did not affect the VEGF-induced internalization of integrin $\beta 1$ (Figure S1). These data indicated that SNX9 is not involved in the internalization of integrin $\beta 1$ from the PM. Secondly, the recycling of integrin $\beta 1$ from early endosomes/recycling endosomes to the PM was measured. As shown (Figure 3g), approximately 40% of integrin $\beta 1$ in the endosomes at time = 0 was recycled back to the PM in the control cells after the 60-min

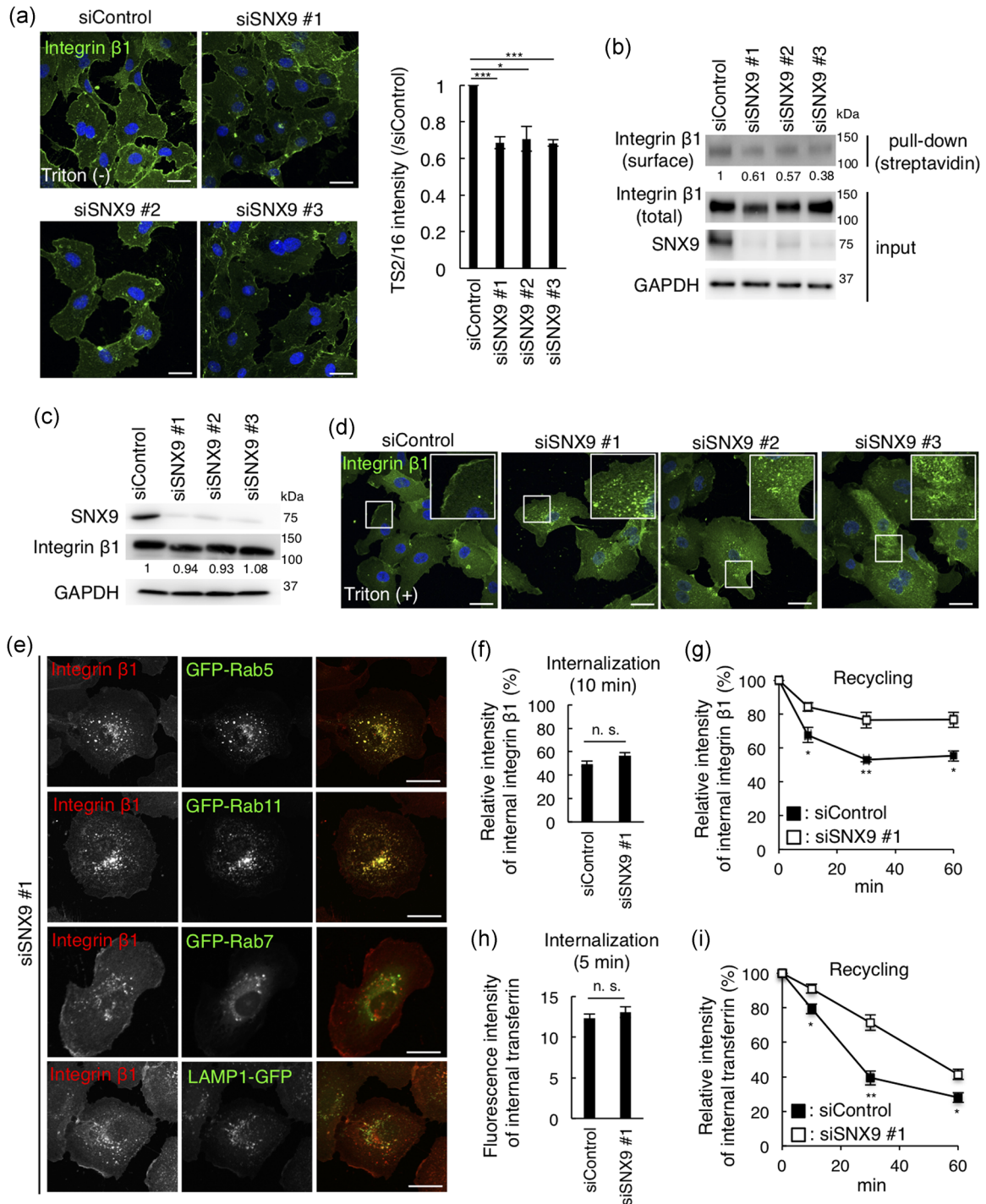


FIGURE 3 Continued.

chase. In contrast, only approximately 20% of integrin $\beta 1$ in the endosomes at time = 0 was recycled back to the PM after the 60-min chase in the cells depleted of SNX9. These results suggested that the SNX9 knockdown significantly delayed the recycling of integrin $\beta 1$ from the endosomes to the PM. We also examined the trafficking of transferrin, which follows the same endocytic recycling pathway as integrin $\beta 1$. We confirmed no difference between the control and SNX9-knockdown cells in the internalization of transferrin (Figure 3h). In contrast, the recycling of transferrin, like that of integrin $\beta 1$, was delayed by the SNX9 knockdown (Figure 3i). Together, SNX9 regulated the recycling of integrin $\beta 1$ from early endosomes/recycling endosomes to the PM in HUVECs, and the defect of recycling of integrin $\beta 1$ may account for the decrease in the level of integrin $\beta 1$ on the cell surface of SNX9-knockdown cells.

Integrin $\beta 1$ on the cell surface is critical for cell migration and cell proliferation (Seguin, Desgrosellier, Weis, & Cheresh, 2015). SNX9 knockdown significantly inhibited the migration of HUVEC on collagen I-coated dishes (Figure S2a). Depletion of SNX9 drastically decreased cell proliferation of HUVEC in a VEGF-independent manner (Figure S2b). These data suggested that SNX9 regulates fundamental endothelial functions in HUVEC.

3.4 | SNX9 expression profiles in tumor endothelial cells in human colorectal cancer tissues

Finally, we sought to clinically validate the functions of SNX9 in endothelial cells. It is well known that the activity of tumor angiogenesis in colorectal cancer is extremely high compared to various other cancers (Mathonnet et al., 2014). Since SNX9 positively regulates tube formation that mimics *in vivo* angiogenesis in HUVECs, we hypothesized that the expression of SNX9 protein is high in tumor endothelial cells in the human colorectal cancer tissues. We first confirmed that the anti-SNX9 antibody was suitable for immunohistochemistry of the human colorectal cancer tissues, by the

absorption experiments. By pre-incubation of the anti-SNX9 antibody with biotinylated recombinant full-length SNX9 or the LC-PX domain of SNX9, in which the antigen for the anti-SNX9 antibody is included, the staining for SNX9 was diminished (Figure 4a,b). In contrast, by preincubation of the anti-SNX9 antibody with biotinylated recombinant LC domain-deleted SNX9 (Δ LC), in which the amino acid sequence targeted by the anti-SNX9 antibody is excluded, the staining for SNX9 was detected (Figure 4a,b). These data suggested that the anti-SNX9 antibody recognized the SNX9 protein in the human colorectal cancer tissues.

We then examined the protein expression of SNX9 in tumor endothelial cells in human colorectal cancer tissues. A total of 57 individual tumor tissues from patients with colorectal cancer were subjected to immunohistochemistry. As shown in Figure 4c, less staining for SNX9 was observed in CD31⁺-endothelial cells (yellow arrows) in the normal colorectal tissues. In contrast, the high-level expression of SNX9 protein was detected in CD31⁺-tumor endothelial cells (Figure 4c; yellow arrowheads) in the human colorectal cancer tissues (Figure 4c). The protein expression of SNX9 in tumor endothelial cells was detected regardless of stage, histological grade, the location of the tumor, and level of invasion in individual colorectal cancer tissues from 57 human patients (Table 2). The expression of SNX9 protein was detected in tumor endothelial cells in the colorectal cancer tissues through stages I, II, III, and IV (Table 2). More than 75% of colorectal cancer tissues (stages II, III, and IV) exhibited staining for SNX9 in tumor endothelial cells. SNX9 was expressed in tumor endothelial cells of well, moderately, and poorly differentiated colorectal cancer tissues (Table 2). In this study, we collected only one mucinous type colorectal cancer tissue, in which the SNX9 expression in tumor endothelial cells was negative. We also classified the colorectal cancer tissues by the location of tumors. SNX9 was expressed in tumor endothelial cells in more than 65% of colorectal cancer tissues regardless of their location in the colon, except for the appendix vermiformis. In this study, we collected only one colorectal

FIGURE 3 SNX9 regulates localization of cell surface integrin $\beta 1$ and the recycling pathway of the cargo in HUVECs. (a) Confocal images and the quantitation of HUVECs fixed after 72 hr transfection of siRNA and stained for integrin $\beta 1$ by Alexa488-conjugated TS2/16, without membrane permeabilization. Bars, 20 μ m. Fifty cells from three independent experiments were analyzed. Data shown are the mean \pm SEM. *** p < .001; * p < .05. (b) Surface proteins were biotinylated, collected with streptavidin beads, and the total and cell surface integrin $\beta 1$ were detected by TS2/16. The numbers indicate the band intensity of surface/total integrin $\beta 1$ (normalized to siControl). (c) Western blots of HUVEC lysates 72 hr posttransfection of siRNAs. The numbers indicate the band intensity of total integrin $\beta 1$ /GAPDH (normalized to siControl). (d) Confocal images of HUVECs fixed after 72 hr transfection of siRNA, permeabilized, and stained for integrin $\beta 1$ by P5D2. Bars, 20 μ m. Inset: magnifications of the squared areas. (e) Confocal images of SNX9 knockdown HUVECs expressing the GFP-tagged organelle markers: Rab5 (early endosomes), Rab11 (recycling endosomes), Rab7 (late endosomes), and LAMP1 (lysosomes) by lentiviral infection. Bars, 20 μ m. (f) Internalization of integrin $\beta 1$. HUVECs were treated with control siRNA and SNX9 siRNA #1 for 72 hr. Surface integrin $\beta 1$ was labeled with Alexa488-TS2/16 and chased in medium for 10 min. The fluorescence intensity of Alexa488-TS2/16 is shown as a percentage of that at 0 min (the fluorescence intensity on the cell surface before quenching). Fifty cells from three independent experiments were analyzed. Data shown are the mean \pm SEM. n. s., not significant. (g) Recycling of integrin $\beta 1$. HUVECs were treated with the control siRNA and SNX9 siRNA #1 for 72 hr. The fluorescence intensity of Alexa488-TS2/16 is shown as a percentage of that at 0 min. Fifty cells from three independent experiments were analyzed. Data shown are the mean \pm SEM. **, p < .01; *, p < .05. (h) Internalization of transferrin. The HUVECs were treated with the control siRNA and SNX9 siRNA #1 for 72 hr. The cells were incubated with Alexa488-Tfn for 5 min, acid-washed, and fixed. The fluorescence intensity of Alexa488-Tfn is shown. Fifty cells from three independent experiments were analyzed. Data shown are the mean \pm SEM. n. s., not significant. (i) Recycling of transferrin. The HUVECs were treated with control siRNA and SNX9 siRNA #1 for 72 hr. The fluorescence intensity of Alexa488-Tfn is shown as the percentage of that at 0 min. Fifty cells from three independent experiments were analyzed. Data shown are the mean \pm SEM. ** p < .01; * p < .05. GAPDH: glyceraldehyde 3-phosphate dehydrogenase; HUVEC: human umbilical vein endothelial cells; SEM: standard error of mean; siRNA: small interfering RNA; SNX9: sorting nexin 9 [Color figure can be viewed at wileyonlinelibrary.com]

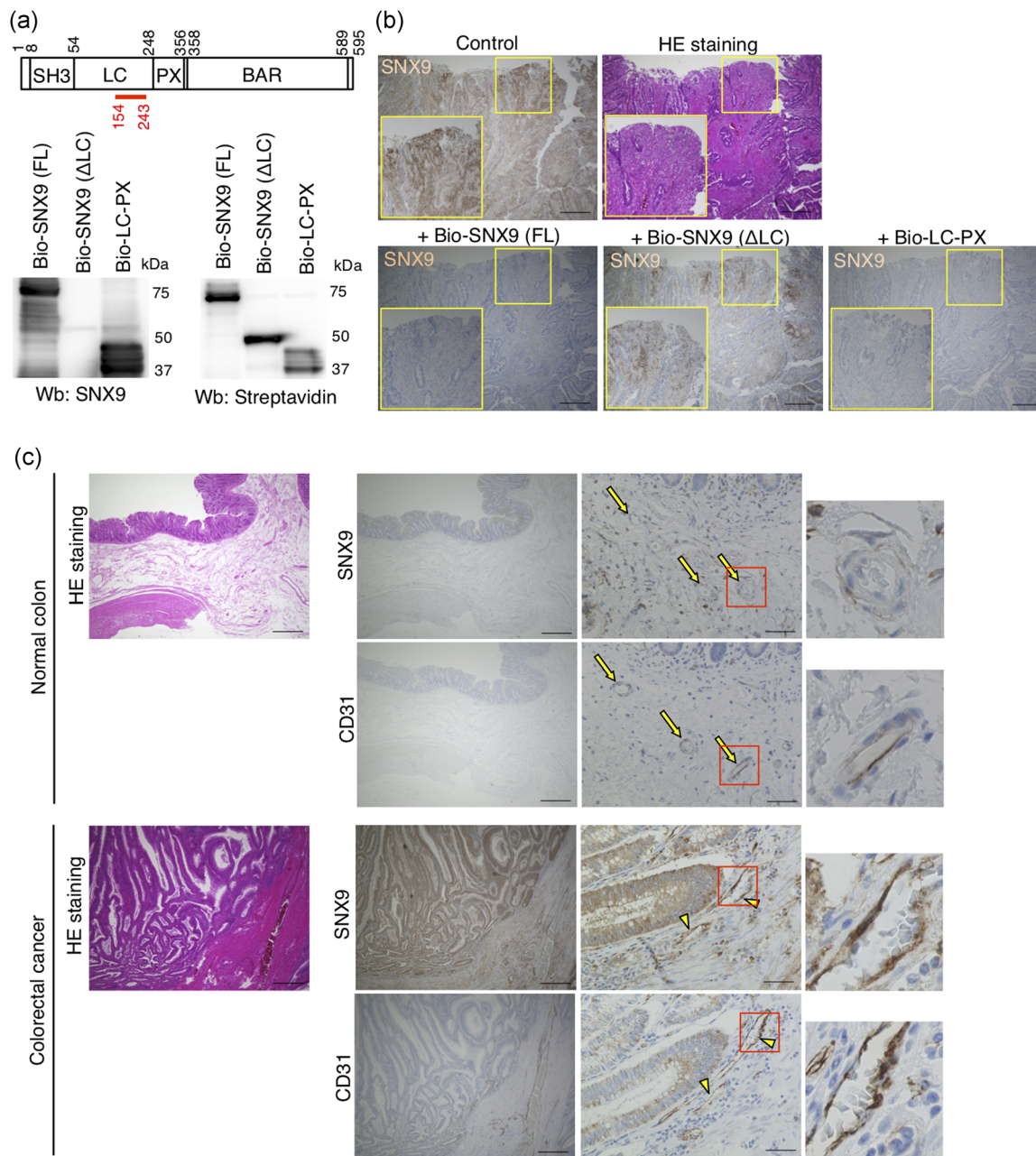


FIGURE 4 Expression of SNX9 in human colorectal cancer tissues. (a) The domain structure of SNX9 and western blot analysis of recombinant biotinylated (Bio-) SNX9 proteins. The numbers in the domain structure represent the order of amino acids from the N-terminus. The red line indicates the location of antigen for the anti-SNX9 antibody used in this study. The anti-SNX9 antibody failed to recognize Bio-SNX9 (Δ LC) recombinant proteins because the antigen amino acid sequence is located in the LC domain. (b) Validation of the anti-SNX9 antibody for immunohistochemistry in the human colorectal cancer tissues. The anti-SNX9 antibody was preincubated with biotinylated full-length SNX9 (Bio-SNX9 [FL]), LC domain-deleted SNX9 (Bio-SNX9 [Δ LC]), or LC-PX domain of SNX9 (Bio-LC-PX). The mixtures of the antibody and recombinant proteins were used as primary antibody. The neighboring sections of a human colorectal cancer tissue were subjected to H&E staining and immunohistological staining for SNX9. Bars, 500 μ m. Inset: magnifications of the yellow squared areas. (c) Representative images of the H&E staining and immunohistological staining for SNX9 and CD31. The neighboring sections of the human normal colon and colorectal cancer tissues were subjected to H&E staining and immunohistochemistry. In normal colon, CD31⁺-endothelial cells are SNX9-negative (yellow arrows). In colorectal cancer tissues, CD31⁺-endothelial cells are SNX9-positive (yellow arrowheads). Bars, 500 μ m (HE staining, left panels of SNX9 and CD31 staining) and 50 μ m (right panels of SNX9 and CD31 staining). Magnifications of the squared areas are shown on the right. H & E: hematoxylin-eosin; SNX9: sorting nexin 9 [Color figure can be viewed at wileyonlinelibrary.com]

cancer tissue from appendix vermiformis, in which the SNX9 expression in tumor endothelial cells was negative. Approximately 80% of colorectal cancer tissues with lymphovascular invasion highly expressed the SNX9 protein in tumor endothelial cells (Table 2). In

regard to the level of invasion, the high-level expression of the SNX9 protein was detected in tumor endothelial cells of more than 65% of T2, T3, and T4 colorectal cancer tissues (Table 2). In this study, we collected only one T1 colorectal cancer tissue, in which the SNX9

TABLE 2 Expression profile of SNX9 protein in human colorectal cancer tissues. Total 57 of human colorectal cancer tissues were subjected to immunohistochemistry for SNX9. The number of human colorectal cancer tissues with SNX9-positive tumor endothelial or epithelial cells were counted. See also Materials and Methods

	Number and percentage of human colorectal cancer tissues	
	With SNX9-positive tumor endothelial cells	With SNX9-positive epithelial cells
Stage		
I	1/3 (33%)	2/3 (67%)
II	17/20 (85%)	17/20 (85%)
III	22/29 (76%)	25/29 (86%)
IV	4/4 (100%)	4/4 (100%)
Histological grade		
Well differentiated	19/22 (86%)	19/22 (86%)
Moderately differentiated	23/30 (77%)	25/30 (83%)
Poorly differentiated (solid type)	2/3 (67%)	3/3 (100%)
Poorly differentiated (non-solid type)	1/1 (100%)	1/1 (100%)
Mucinous	0/1 (0%)	1/1 (100%)
Location of tumor		
Appendix vermiformis	0/1 (0%)	1/1 (100%)
Cecum	2/3 (67%)	3/3 (100%)
Ascending colon	11/13 (85%)	12/13 (92%)
Transverse colon	5/5 (100%)	5/5 (100%)
Descending colon	3/5 (60%)	4/5 (80%)
Sigmoid colon	9/11 (82%)	9/11 (82%)
Rectum	15/19 (79%)	15/19 (79%)
Lymphovascular invasion		
Present	45/56 (80%)	49/56 (88%)
Absent	0/1 (0%)	0/1 (0%)
Level of invasion		
T1	0/1 (0%)	0/1 (0%)
T2	2/3 (67%)	3/3 (100%)
T3	27/34 (79%)	29/34 (85%)
T4	16/19 (84%)	17/19 (89%)

Note. SNX9: sorting nexin 9.

expression in tumor endothelial cells was negative. These data suggested that the high-level expression of SNX9 in tumor endothelial cells might enhance tumor angiogenesis in colorectal tumors, and contribute to the development of colorectal tumors.

3.5 | High expression of SNX9 mRNA significantly correlated with poor prognosis of human colorectal cancer

We noticed that protein expression of SNX9 was high not only in tumor endothelial cells but also in epithelial cells of human colorectal cancer tissues (Figure 4c). Its expression profile was similar to that in tumor endothelial cells (Table 2). These data suggested that SNX9 may also have critical roles in colorectal cancer epithelial cells, and SNX9 expression could determine the prognosis of human colorectal cancers. We thus examined if the expression level of SNX9 correlates with the prognosis of human colorectal cancers using the GEO

datasets (accession numbers GSE14333 and GSE17536; Jorissen et al., 2009; Smith et al., 2010). We found that the high mRNA expression of SNX9 significantly correlated with poor prognosis for both the overall survival and disease-free survival of patients with colorectal cancers (Figure 5; $p = .003$; high: $n = 99$, low: $n = 78$; $p < .0001$, high: $n = 25$, low: $n = 201$, respectively). These data suggested that SNX9 functions as an oncogenic gene in the development of human colorectal cancers.

4 | DISCUSSION

SNX9 is a multifunctional protein which regulates endocytosis (e.g., clathrin-mediated endocytosis, clathrin-independent endocytosis, macropinocytosis), cell migration, cell invasion, and cell division (Bendris & Schmid, 2017). In the present study, we found that SNX9 regulates the recycling of cargos (integrin $\beta 1$, transferrin) from early/recycling endosomes to the plasma membrane in HUVECs (Figure 2e–i). In the process of clathrin-mediated endocytosis, SNX9 is recruited to clathrin-coated pits by the recognition of membrane curvature and phosphoinositides (Daste et al., 2017; Schoneberg et al., 2017). SNX9 in the clathrin-coated pits facilitates the recruitment and/or activation of dynamin, which catalyzes membrane fission from the plasma membrane (Schoneberg et al., 2017). In the process of recycling of cargos such as integrin $\beta 1$ and transferrin from early/recycling endosomes, SNX9 may also function in the membrane scission from early or/and recycling endosomes in HUVECs.

Recently, SNX9 has been shown to regulate invadopodia formation and cell invasion in breast cancer cells (Bendris, Stearns, et al., 2016; Bendris, Williams, et al., 2016). SNX9 enhances the internalization of membrane-type-1 matrix metalloproteinase (MT1-MMP) from the plasma membrane, which negatively regulates the invadopodia formation (Bendris, Stearns, et al., 2016). Loss of SNX9 increased the surface level of a disintegrin and metalloprotease 9 (ADAM9) owing to the inhibition of endocytosis of ADMA9, resulting in the increase in shedding of Ephrin receptor B4 at the plasma membrane (Mygind et al., 2018). SNX9 is also required for cell migration through the inhibition of the RhoA-Rho-associated protein kinase pathway (Bendris, Williams, et al., 2016). Pathologically, its protein expression is lowered in primary breast cancer tumors and upregulated in metastatic breast cancer tumors (Bendris, Stearns, et al., 2016; Bendris, Williams, et al., 2016). In contrast to the protein expression profile of SNX9 in human breast cancer tissues, we found that the SNX9 protein was expressed in both epithelial and endothelial cells of human colorectal cancer tissues regardless of their pathological characteristics (Table 2). SNX9 may also function in cell invasion/migration in the epithelial cells of colorectal cancers, in addition to its novel function in angiogenesis of the endothelial cells revealed in this study. Clinically, the recent meta-analysis with more than 1.4 million patients with colorectal cancer showed that the risk of patient death with left-sided primary colon tumor was 20% lower than patients with right-sided primary colon tumor (Petrelli et al., 2016). The SNX9 expression in both the epithelial and endothelial

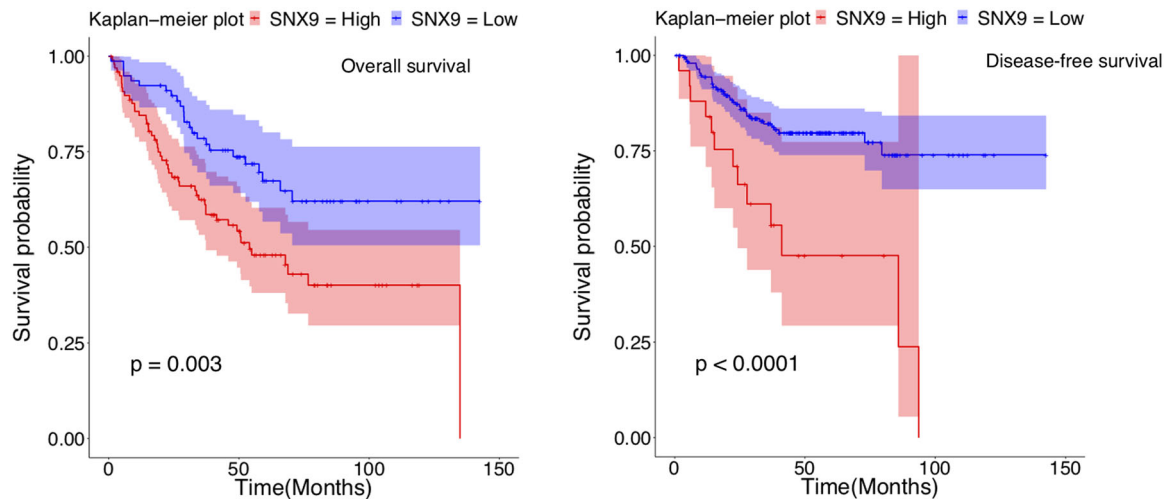


FIGURE 5 Survival analysis with SNX9 expression profiles in human colorectal cancers. The Kaplan–Meier plot with SNX9 expression profiles in GSE17536 and GSE14333 datasets using endpoint overall survival status (left) and endpoint disease-free survival status (right). Shading along the curve showed 95% confidential interval. In human colorectal cancers, the high expression of SNX9 was correlated to poor prognosis for overall survival (high: $n = 99$; low: $n = 78$) and disease-free survival (high: $n = 25$; low: $n = 201$). SNX9: sorting nexin 9 [Color figure can be viewed at wileyonlinelibrary.com]

cells in the colorectal cancer tissues was positive regardless of the tumor location (Table 2), suggesting that SNX9 is not likely to be involved in the determination of prognostic differences between the left-sided and right-sided colorectal tumors. The upregulation of SNX9 protein in breast and colorectal cancer tissues could be due to the inhibition of its protein degradation and/or enhancement of its transcription. The E3 ubiquitin ligase Itch has a potential to ubiquitinate SNX9, leading to its degradation in the HEK293 cells (Baumann, Lindholm, Rimoldi, & Levy, 2010). The transcription factor STAT5B is required for the transcription of SNX9 mRNA in human CD4⁺T cells (Kanai et al., 2014). The regulatory mechanisms for SNX9 protein expression in endothelial cells and cancer cells would be investigated in the future.

Our siRNA screening against 33 SNX genes showed that knockdown of sorting nexin 5 (SNX5) also inhibited tube formation of HUVEC (Figure 1). SNX5 knockdown affected neither protein expression, cellular localization nor the surface level of integrin $\beta 1$ (Figure S3). How SNX5 is involved in tube formation is unknown. Other members of sorting nexin family, sorting nexin 1 (SNX1) and sorting nexin 10 (SNX10) have been shown to act as tumor suppressors of colorectal cancers (Bian et al., 2016; Huang et al., 2011; Le et al., 2018; Nguyen et al., 2006; Zhang et al., 2018). Both mRNA and protein levels of SNX1 were significantly decreased in human colorectal cancer tissues (Nguyen et al., 2006). SNX1 knockdown showed increased proliferation and decreased apoptosis in colorectal cancer cells (Nguyen et al., 2006). SNX10 expression was also decreased in human colorectal cancer tissues (Zhang et al., 2018). Depletion of SNX10 promoted mouse colorectal tumor formation and cell proliferation/survival in human colorectal cancer cells owing to increased mammalian target of rapamycin activation through chaperone-mediated autophagy (Le et al., 2018; Zhang et al., 2018). In contrast to SNX1 and SNX10 as antioncogenic genes, our present study suggested that SNX9 is an oncogenic gene of colorectal cancers. SNX1 positively regulates

endocytosis of epidermal growth factor receptor (EGFR) and over-expression of SNX1 reduced the cell surface levels of EGFR (Kurten, Cadena, & Gill, 1996). Here, we showed that SNX9 is essential for the recycling of integrin $\beta 1$ and that knockdown of SNX9 reduced the cell surface levels of integrin $\beta 1$. The distinct site of action of individual SNXs, i.e., endocytosis from the PM or recycling traffic from endosomes, may dictate their different roles in tumorigenesis.

Integrins are receptors on the plasma membrane for cell adhesion to the extracellular matrices such as fibronectin and collagen (Hynes, 2002). The α and β subunits of integrins noncovalently form heterodimers (Paul, Jacquemet, & Caswell, 2015). Accumulated evidence have shown that angiogenesis requires proper cellular adhesion of endothelial cells to the extracellular matrix, which is mediated by the cell surface integrins (Carmeliet & Jain, 2011). Inhibitory antibodies and peptides for integrin $\alpha 1/\beta 1$, $\alpha 2/\beta 1$, and $\alpha 5/\beta 1$ suppressed angiogenesis (Kim, Bell, Mousa, & Varner, 2000; Senger et al., 1997). Pathologically, the inhibitory antibodies for integrin $\alpha 1/\beta 1$ and $\alpha 2/\beta 1$ also reduced the tumor angiogenesis and tumor growth of human squamous cell carcinoma xenografts (Senger et al., 2002). The combination of 5-fluorouracil infusion and the inhibition of integrin $\alpha 5/\beta 1$ by a small peptide (ATN-161) reduced the colorectal liver metastasis (Stoeltzing et al., 2003). Although the concept that the inhibition of integrin $\beta 1$ leads to the suppression of angiogenesis has been proved both in vitro and in vivo, to date, inhibitory antibodies and antagonizing peptides targeting the cell surface integrin $\beta 1$ have not been successfully developed as antiangiogenic drugs for the cancer therapy. In the present study, we identified SNX9 as a novel angiogenic factor that regulates the recycling pathway of integrin $\beta 1$. Other molecules that regulate integrin $\beta 1$ recycling such as Arf6 and CUL3/ANKFY1 complex are also essential for angiogenesis (Hongu et al., 2015; Maekawa et al., 2017). The machinery of integrin $\beta 1$ trafficking could also be targets for the development of novel antiangiogenic drugs.

ACKNOWLEDGEMENTS

The authors thank Ms. Ayako Fujisaki, Ms. Mami Chosei, Ms. Yuki Tanaka, Dr. Tomohisa Sakaue, Dr. Shinji Fukuda, Dr. Hirotaka Takahashi, Dr. Hiroyuki Takeda, and Dr. Tatsuya Sawasaki (Ehime University) for their technical assistance. This study was supported by JSPS KAKENHI grant number JP18K16317 to K. T. and JP18K15244, YOKOYAMA Foundation for Clinical Pharmacology 2017 (YRY-1703) to MM and JSPS KAKENHI grant number JP16H046980 to S. H. This investigation was supported in parts by The Mochida Memorial Foundation for Medical and Pharmaceutical Research to M.M.

CONFLICT OF INTERESTS

The authors declare that there are no conflict of interests.

AUTHOR CONTRIBUTIONS

K. T. and M. M. designed and performed the experiments, analyzed the data, interpreted the results, and wrote the paper. T. K. and J. N. performed the experiments. R. K., S. K., S. A., M. Y., and K. I. collected the human samples. K. S., T. T., and Y. W. analyzed the data. S. K., J. N., K. S., T. T., Y. W., and S. H. designed the experiments, interpreted the results, and wrote the paper.

ORCID

Masashi Maekawa  <http://orcid.org/0000-0002-9574-1906>

REFERENCES

- Arjonen, A., Alanko, J., Veltel, S., & Ivaska, J. (2012). Distinct recycling of active and inactive beta1 integrins. *Traffic*, *13*(4), 610–625.
- Arnaoutova, I., & Kleinman, H. K. (2010). In vitro angiogenesis: Endothelial cell tube formation on gelled basement membrane extract. *Nature Protocols*, *5*(4), 628–635.
- Baumann, C., Lindholm, C. K., Rimoldi, D., & Lévy, F. (2010). The E3 ubiquitin ligase Itch regulates sorting nexin 9 through an unconventional substrate recognition domain. *The FEBS journal*, *277*(13), 2803–2814.
- Bendris, N., & Schmid, S. L. (2017). Endocytosis, metastasis and beyond: multiple facets of snx9. *trends in cell biology*, *27*(3), 189–200.
- Bendris, N., Stearns, C. J. S., Reis, C. R., Rodriguez-Canales, J., Liu, H., Witkiewicz, A. W., ... Schmid, S. L. (2016). Sorting nexin 9 negatively regulates invadopodia formation and function in cancer cells. *Journal of Cell Science*, *129*(14), 2804–2816.
- Bendris, N., Williams, K. C., Reis, C. R., Welf, E. S., Chen, P. H., Lemmers, B., ... Schmid, S. L. (2016). SNX9 promotes metastasis by enhancing cancer cell invasion via differential regulation of RhoGTPases. *Molecular Biology of the Cell*, *27*, 1409–1419.
- Bergers, G., & Hanahan, D. (2008). Modes of resistance to anti-angiogenic therapy. *Nature Reviews Cancer*, *8*(8), 592–603.
- Bian, Z., Feng, Y., Xue, Y., Hu, Y., Wang, Q., Zhou, L., ... Huang, Z. (2016). Down-regulation of SNX1 predicts poor prognosis and contributes to drug resistance in colorectal cancer. *Tumour Biology*, *37*(5), 6619–6625.
- Carmeliet, P., & Jain, R. K. (2011). Molecular mechanisms and clinical applications of angiogenesis. *Nature*, *473*(7347), 298–307.
- Clarke, J. M., & Hurwitz, H. I. (2013). Understanding and targeting resistance to anti-angiogenic therapies. *Journal of Gastrointestinal Oncology*, *4*(3), 253–263.
- Cullen, P. J. (2008). Endosomal sorting and signalling: An emerging role for sorting nexins. *Nature Reviews Molecular Cell Biology*, *9*(7), 574–582.
- Daste, F., Walrant, A., Holst, M. R., Gadsby, J. R., Mason, J., Lee, J. E., ... Gallop, J. L. (2017). Control of actin polymerization via the coincidence of phosphoinositides and high membrane curvature. *Journal of Cell Biology*, *216*(11), 3745–3765.
- De Falco, S. (2014). Antiangiogenesis therapy: An update after the first decade. *The Korean Journal of Internal Medicine*, *29*(1), 1–11.
- De Franceschi, N., Hamidi, H., Alanko, J., Sahgal, P., & Ivaska, J. (2015). Integrin traffic—the update. *Journal of Cell Science*, *128*(5), 839–852.
- Ferrara, N., & Adamis, A. P. (2016). Ten years of anti-vascular endothelial growth factor therapy. *Nature Reviews Drug Discovery*, *15*(6), 385–403.
- Hida, K., Maishi, N., Annan, D., & Hida, Y. (2018). Contribution of Tumor Endothelial Cells in Cancer Progression. *International Journal of Molecular Sciences*, *19*(5), 1272.
- Hongu, T., Funakoshi, Y., Fukuhara, S., Suzuki, T., Sakimoto, S., Takakura, N., ... Kanaho, Y. (2015). Arf6 regulates tumour angiogenesis and growth through HGF-induced endothelial beta1 integrin recycling. *Nature Communications*, *6*, 7925.
- Horowitz, A., & Seerapu, H. R. (2012). Regulation of VEGF signaling by membrane traffic. *Cellular Signalling*, *24*(9), 1810–1820.
- Huang, Z., Huang, S., Wang, Q., Liang, L., Ni, S., Wang, L., ... Du, X. (2011). MicroRNA-95 promotes cell proliferation and targets sorting Nexin 1 in human colorectal carcinoma. *Cancer Research*, *71*(7), 2582–2589.
- Hynes, R. O. (2002). Integrins: Bidirectional, allosteric signaling machines. *Cell*, *110*(6), 673–687.
- de Jesus-Gonzalez, N., Robinson, E., Moslehi, J., & Humphreys, B. D. (2012). Management of antiangiogenic therapy-induced hypertension. *Hypertension*, *60*(3), 607–615.
- Jorissen, R. N., Gibbs, P., Christie, M., Prakash, S., Lipton, L., Desai, J., ... Sieber, O. M. (2009). Metastasis-associated gene expression changes predict poor outcomes in patients with dukes stage B and C colorectal cancer. *Clinical Cancer Research*, *15*(24), 7642–7651.
- Kanai, T., Seki, S., Jenks, J. A., Kohli, A., Kawli, T., Martin, D. P., ... Nadeau, K. C. (2014). Identification of STAT5A and STAT5B target genes in human T cells. *PLoS One*, *9*(1), e86790.
- Kandachar, V., & Roegiers, F. (2012). Endocytosis and control of Notch signaling. *Current Opinion in Cell Biology*, *24*(4), 534–540.
- Kim, S., Bell, K., Mousa, S. A., & Varner, J. A. (2000). Regulation of angiogenesis in vivo by ligation of integrin alpha5beta1 with the central cell-binding domain of fibronectin. *The American Journal of Pathology*, *156*(4), 1345–1362.
- Kiyoi, T. (2018). Histological analysis of arthritic joints. *Methods in Molecular Biology*, *1868*, 29–39.
- Kurten, R. C., Cadena, D. L., & Gill, G. N. (1996). Enhanced degradation of EGF receptors by a sorting nexin, SNX1. *Science*, *272*(5264), 1008–1010.
- Le, Y., Zhang, S., Ni, J., You, Y., Luo, K., Yu, Y., & Shen, X. (2018). Sorting nexin 10 controls mTOR activation through regulating amino-acid metabolism in colorectal cancer. *Cell Death & Disease*, *9*(6), 666.
- Lee, S., Uchida, Y., Wang, J., Matsudaira, T., Nakagawa, T., Kishimoto, T., ... Arai, H. (2015). Transport through recycling endosomes requires EHD1 recruitment by a phosphatidyserine translocase. *EMBO Journal*, *34*(5), 669–688.
- Lupo, G., Caporarello, N., Olivieri, M., Cristaldi, M., Motta, C., Bramanti, V., ... Anfuso, C. D. (2016). Anti-angiogenic therapy in cancer: Downsides and new pivots for precision medicine. *Frontiers in Pharmacology*, *7*, 519.
- Maekawa, M., Tanigawa, K., Sakaue, T., Hiyoshi, H., Kubota, E., Joh, T., ... Higashiyama, S. (2017). Cullin-3 and its adaptor protein ANKFY1 determine the surface level of integrin beta1 in endothelial cells. *Biology Open*, *6*(11), 1707–1719.
- Maes, H., Olmeda, D., Soengas, M. S., & Agostinis, P. (2016). Vesicular trafficking mechanisms in endothelial cells as modulators of the tumor vasculature and targets of antiangiogenic therapies. *The FEBS Journal*, *283*(1), 25–38.

- Maishi, N., & Hida, K. (2017). Tumor endothelial cells accelerate tumor metastasis. *Cancer Prevention Research*, 108(10), 1921–1926.
- Mathonnet, M., Perraud, A., Christou, N., Akil, H., Melin, C., Battu, S., ... Denizot, Y. (2014). Hallmarks in colorectal cancer: Angiogenesis and cancer stem-like cells. *World Journal of Gastroenterology*, 20(15), 4189–4196.
- Mellman, I., & Yarden, Y. (2013). Endocytosis and cancer. *Cold Spring Harbor Perspectives in Biology*, 5(12), a016949–a016949.
- Murakami, A., Maekawa, M., Kawai, K., Nakayama, J., Araki, N., Semba, K., ... Higashiyama, S. (2019). Cullin-3/KCTD10 E3 complex is essential for Rac1 activation through RhoB degradation in human epidermal growth factor receptor 2-positive breast cancer cells. *Cancer Prevention Research*, 110(2), 650–661.
- Mygind, K. J., Störko, T., Freiberg, M. L., Samsøe-Petersen, J., Schwarz, J., Andersen, O. M., & Kveiborg, M. (2018). Sorting nexin 9 (SNX9) regulates levels of the transmembrane ADAM9 at the cell surface. *Journal of Biological Chemistry*, 293(21), 8077–8088.
- Nguyen, L. N., Holdren, M. S., Nguyen, A. P., Furuya, M. H., Bianchini, M., Levy, E., ... Parks, W. T. (2006). Sorting nexin 1 down-regulation promotes colon tumorigenesis. *Clinical Cancer Research*, 12(23), 6952–6959.
- Ohnuki, H., Inoue, H., Takemori, N., Nakayama, H., Sakaue, T., Fukuda, S., ... Higashiyama, S. (2012). BAZF, a novel component of cullin3-based E3 ligase complex, mediates VEGFR and Notch cross-signaling in angiogenesis. *Blood*, 119(11), 2688–2698.
- Paul, N. R., Jacquemet, G., & Caswell, P. T. (2015). Endocytic trafficking of integrins in cell migration. *Current Biology*, 25(22), R1092–R1105.
- Petrelli, F., Tomasello, G., Borgonovo, K., Ghidini, M., Turati, L., Dallera, P., & Barni, S. (2016). Prognostic survival associated with left-sided vs right-sided colon cancer: A systematic review and meta-analysis. *JAMA Oncology*.
- Potente, M., Gerhardt, H., & Carmeliet, P. (2011). Basic and therapeutic aspects of angiogenesis. *Cell*, 146(6), 873–887.
- Saltz, L. B., Clarke, S., Díaz-Rubio, E., Scheithauer, W., Figuree, A., Wong, R., ... Cassidy, J. (2008). Bevacizumab in combination with oxaliplatin-based chemotherapy as first-line therapy in metastatic colorectal cancer: A randomized phase III study. *Journal of Clinical Oncology*, 26(12), 2013–2019.
- Schöneberg, J., Lehmann, M., Ullrich, A., Posor, Y., Lo, W. T., Lichtner, G., ... Noé, F. (2017). Lipid-mediated PX-BAR domain recruitment couples local membrane constriction to endocytic vesicle fission. *Nature Communications*, 8, 15873.
- Seguin, L., Desgrosellier, J. S., Weis, S. M., & Cheresch, D. A. (2015). Integrins and cancer: Regulators of cancer stemness, metastasis, and drug resistance. *Trends in Cell Biology*, 25(4), 234–240.
- Senger, D. R., Claffey, K. P., Benes, J. E., Perruzzi, C. A., Sergiou, A. P., & Detmar, M. (1997). Angiogenesis promoted by vascular endothelial growth factor: Regulation through alpha1beta1 and alpha2beta1 integrins. *Proceedings of the National Academy of Sciences of the United States of America*, 94(25), 13612–13617.
- Senger, D. R., Perruzzi, C. A., Streit, M., Kotliansky, V. E., de Fougères, A. R., & Detmar, M. (2002). The alpha(1)beta(1) and alpha(2)beta(1) integrins provide critical support for vascular endothelial growth factor signaling, endothelial cell migration, and tumor angiogenesis. *The American Journal of Pathology*, 160(1), 195–204.
- Sherwood, L. M., Parris, E. E., & Folkman, J. (1971). Tumor angiogenesis: Therapeutic implications. *The New England Journal of Medicine*, 285(21), 1182–1186.
- Sliesoraitis, S., & Tawfik, B. (2011). Bevacizumab-induced bowel perforation. *The Journal of the American Osteopathic Association*, 111(7), 437–441.
- Smith, J. J., Deane, N. G., Wu, F., Merchant, N. B., Zhang, B., Jiang, A., ... Beauchamp, R. D. (2010). Experimentally derived metastasis gene expression profile predicts recurrence and death in patients with colon cancer. *Gastroenterology*, 138(3), 958–968.
- Stoeltzing, O., Liu, W., Reinmuth, N., Fan, F., Parry, G. C., Parikh, A. A., ... Ellis, L. M. (2003). Inhibition of integrin alpha5beta1 function with a small peptide (ATN-161) plus continuous 5-FU infusion reduces colorectal liver metastases and improves survival in mice. *International Journal of Cancer*, 104(4), 496–503.
- Zhang, S., Hu, B., You, Y., Yang, Z., Liu, L., Tang, H., ... Shen, X. (2018). Sorting nexin 10 acts as a tumor suppressor in tumorigenesis and progression of colorectal cancer through regulating chaperone mediated autophagy degradation of p21(Cip1/WAF1). *Cancer Letters*, 419, 116–127.

SUPPORTING INFORMATION

Additional supporting information may be found online in the Supporting Information section at the end of the article.

How to cite this article: Tanigawa K, Maekawa M, Kiyoi T, et al. SNX9 determines the surface levels of integrin $\beta 1$ in vascular endothelial cells: Implication in poor prognosis of human colorectal cancers overexpressing SNX9. *J Cell Physiol*. 2019;234:17280–17294. <https://doi.org/10.1002/jcp.28346>